Two-Paralleled PWM Power Amplifiers to Generate Highly Precise Gradient Magnetic Fields in MRI Systems

Shuji Watanabe*, Prasanna Boyagoda*, Hiroshi Takano**, Mutsuo Nakaoka*

*The Graduate School of Engineering & Science,
Yamaguchi University, Yamaguchi, 755-8611, JAPAN

**Hitachi Medical Corporation, Kashiwa, 277-0804, JAPAN

ABSTRACT – This paper presents a two-paralleled 4 quadrant DC chopper type PWM power conversion circuit in order to generate a gradient magnetic field in the Magnetic Resonance Imaging (MRI) system. This power amplifier is connected in parallel with the conventional 4-quadrant DC chopper using IGBTs at their inputs/outputs to realize further high-power density, high speed current tracking control, and to get a low switching ripple amplitude in a controlled current in the Gradient Coils (GCs). Moreover, the power conversion circuit has to realize quick rise/fall response characteristics in proportion to various target currents in GCs.

It is proposed in this paper that a unique control scheme can achieve the above objective. DSP-based control systems realize a high control facility and accuracy. It is proved that the new control system will greatly enlarge the diagnostic target and improve the image quality of MRI.

1. INTRODUCTION

The MRI system needs a medical office detecting a disease in early stages. It has good points which is possible to take any section picture in human body, unnecessary to give consideration to side effects for the X-ray. The MRI system can get any image in human body, since the hydrogen in the body radiates radio waves from a resonance with changing magnetic fields. To realize high-speed imaging, various currents in GCs have higher output amplitude and quick rise and fall response capabilities.

Considering this backdrop, a new power conversion circuit for switch-mode gradient power amplifiers in MRI systems is proposed in this paper using a parallel connection of the 4 quadrant DC chopper circuit with IGBTs at their inputs/outputs (Fig.1), and a unique digital control scheme for the circuit on the basis of optimal type-1 servo control. Furthermore, preview digital control is introduced into the amplifier with a corrective control scheme applied to improve the control of GC current and attain robustness. The effectiveness of the above scheme is evaluated through computer-aided analysis.

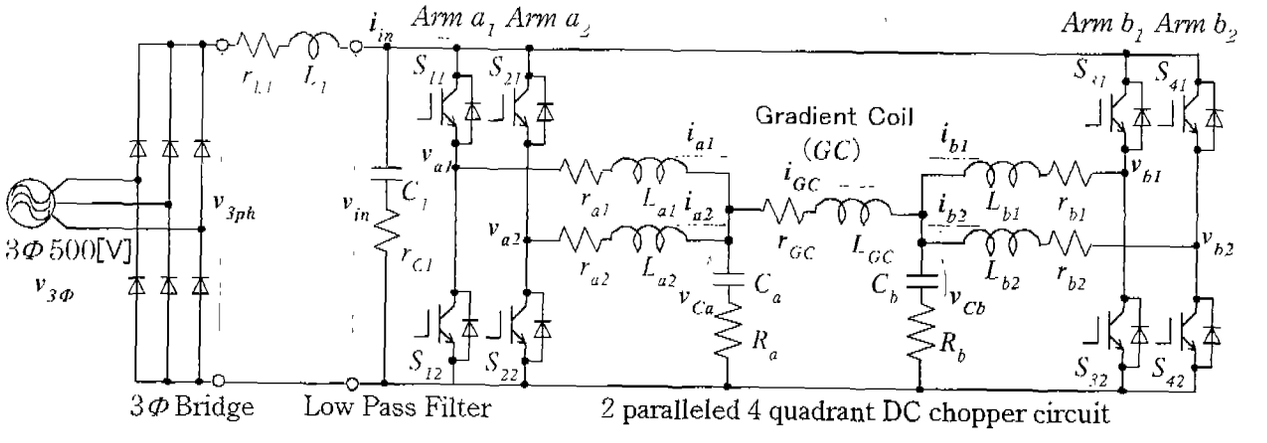

Fig.1 The parallel connection of the 4 quadrant DC chopper circuit with IGBTs

2. OPTIMAL PULSE LAYOUT FOR IGBT GATE SIGNAL IN PROPOSED CIRCUIT

The discrete system state equation of the power conversion circuit shown in Fig.1 can be written as

$$\begin{aligned} \boldsymbol{x}(k+1) &= \boldsymbol{A}\boldsymbol{x}(k) + \boldsymbol{B}\boldsymbol{u}(k-1) \\ \boldsymbol{y}(k) &= \boldsymbol{C}\boldsymbol{x}(k) \end{aligned} \tag{1}$$

where $\boldsymbol{x}(k)=[i_{a1}(k),\ i_{a2}(k),\ i_{b1}(k),\ i_{b2}(k),\ v_{Ca}(k),\ v_{Cb}(k),\ i_{GC}(k)]^T \in \boldsymbol{R}^{7\cdot1}$, is the system state vector, $\boldsymbol{u}(k-1)=[v_{a1}\cdot p_1(k-1),\ v_{a2}\cdot p_2(k-1),\ v_{b1}\cdot p_3(k-1),\ v_{b2}\cdot p_4(k-1)]^T \in \boldsymbol{R}^{4\cdot1}$ is the system input vector, and $\boldsymbol{y}(k)=[i_{a1}(k),\ i_{a2}(k),\ i_{b1}(k),\ i_{b2}(k)]^T \in \boldsymbol{R}^{4\cdot1}$ is the system output vector. $\boldsymbol{A}$, $\boldsymbol{B}$, and $\boldsymbol{C}$ are real coefficient matrices with appropriate dimensions. Since digital control involves a time lag, it is necessary for the DSPs to consider the calculating time. Therefore, the input signal $\boldsymbol{u}(k-1)$ is calculated between the sampling time k-1 and k.

The power switch devices are turned on and off such that the input voltages to each of the LCR filters are given some pulses with magnitude v_{in} or 0 and width $p_i(k)$ (i = 1 to 4) centered during sampling interval T_S. The pulse width vector $\boldsymbol{p}(k)=[p_1(k),\ p_2(k),\ p_3(k),\ p_4(k)]^T \in \boldsymbol{R}^{4\cdot1}$ will be derived in terms of the following equation.

$$\boldsymbol{p}(k) = \frac{\boldsymbol{u}(k)}{v_{in}} \tag{2}$$

Each chopper inductor and capacitor can behave like a low pass filter, but these are not effective enough to eliminate the current ripple. The basic concept of pulse generation procedure to minimize the current ripple is illustrated in Fig.2. Using data sampled at $t=(k-1)T_S$, input vector $\boldsymbol{u}(k)$ is calculated during a sampling interval T_S with the pulses $[p_1(k),\ p_3(k)]$ centered on sampling interval T_S and the pulses $[p_2(k),\ p_4(k)]$ equally divided in half and arranged on each side of the sampling interval T_S. As a result of this pulse generation procedure, the filter inductor currents i_{a1} and i_{a2} (or i_{b1} and i_{b2}) which take the form of triangular-waves are obtained as shown in Fig.2. The ripples of filter inductor currents are mutually canceled out, and thus the ripple of the synthesized current $i_{a1}+i_{a2}$ (or $i_{b1}+i_{b2}$) becomes very small and its frequency is twice as high ($2f_S$) as each of the inductor currents (f_S). The current into the GC may be considered as been produced by the superposition of filter inductor currents i_{a1} and i_{a2} (or i_{b1} and i_{b2}). However a small current will flow through the capacitor and in order to obtain better control of the GC current, it should be taken into consideration.

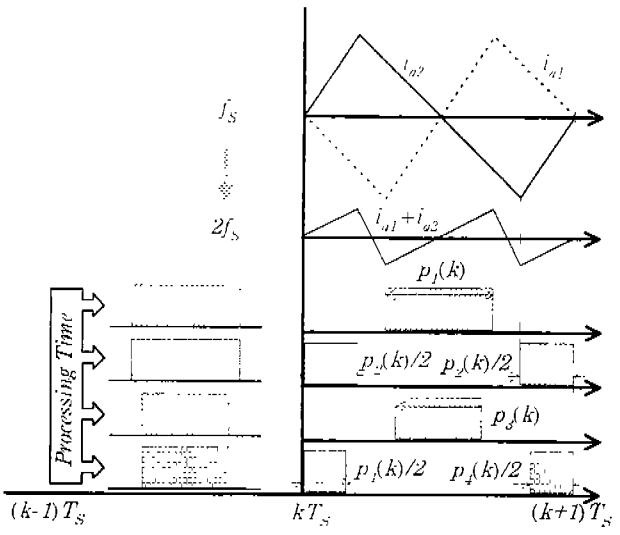

Fig.2 IGBT gate signal layout in the amplifier

3. THE DESIGN OF OPTIMAL TYPE1 DIGITAL CONTROL SYSTEM

Even though the GC current is designed as the combination of two target currents, $\boldsymbol{y}_{ref}$, the GC current will not achieve the desired value since a current flows through the capacitor C_a (or C_b). Usually, the error signal vector is defined as $\boldsymbol{e}(k)=\boldsymbol{y}_{ref}(k)-\boldsymbol{y}(k)$ | $\boldsymbol{e}(k) \in \boldsymbol{R}^{4\cdot1}$, where $\boldsymbol{y}_{ref}(k) \in \boldsymbol{R}^{4\cdot1}$ consists of the output reference signals, but in order to overcome this error, a corrective expression is added as

$$\begin{aligned} \boldsymbol{e}_C(k) &= \boldsymbol{y}_{ref}(k) + \boldsymbol{R}_C(k) - \boldsymbol{y}(k) \\ &= \boldsymbol{y}_{ref\ c}(k) - \boldsymbol{y}(k) \end{aligned} \tag{3}$$

where $\boldsymbol{R}_C(k) = \boldsymbol{F}_C(k)\boldsymbol{x}(k)$

$$\boldsymbol{F}_C(k) = \begin{bmatrix} c_1(k) & 0 & 0 & 0 & 0 & 0 & 0 \\ 0 & c_1(k) & 0 & 0 & 0 & 0 & 0 \\ 0 & 0 & c_2(k) & 0 & 0 & 0 & 0 \\ 0 & 0 & 0 & c_2(k) & 0 & 0 & 0 \end{bmatrix}$$

$$c_1(k) = \frac{i_{a1}(k) + i_{a2}(k) - i_{GC}(k)}{2.0 \times \left(i_{a1}(k) + i_{a2}(k)\right)}$$

$$c_2(k) = \frac{i_{b1}(k) + i_{b2}(k) + i_{GC}(k)}{2.0 \times \left(i_{b1}(k) + i_{b2}(k)\right)}$$

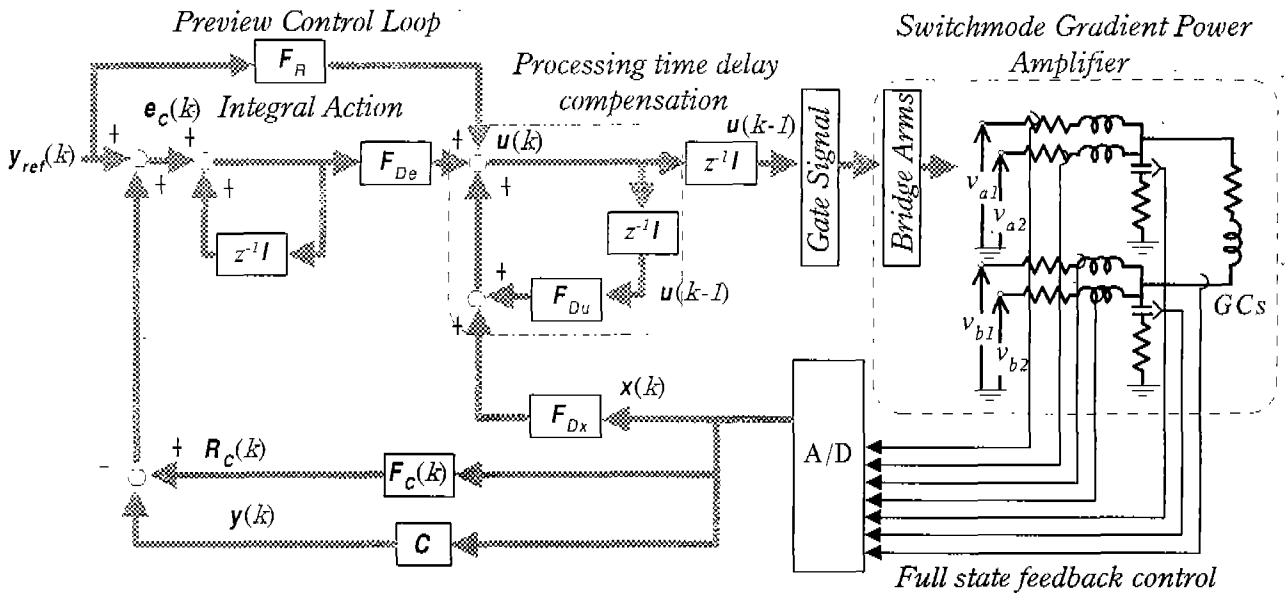

Fig.3 Improved Digital Optimal Type-1 Servo Preview Control system for two paralleled 4 quadrant DC chopper

$R_C(k)$ makes compensation for capacitor current losses of each filter. Since $R_C(k)$ is calculated each sampling time, $e_C(k)$ deals with the difference between each filter current and reference, as usual.

In the design stages, we must take the processing delay time into account and compensate it. Assuming that the processing time, which is regarded as input delay time, is equal to a sampling interval T_S, the Error system is derived from (3).

$$\begin{bmatrix} e_C(k+1) \\ \Delta x(k+1) \\ \Delta u(k) \end{bmatrix} = \begin{bmatrix} I_4 & -CA & -CB \\ 0 & A & B \\ 0 & 0 & 0 \end{bmatrix} \begin{bmatrix} e_C(k) \\ \Delta x(k) \\ \Delta u(k-1) \end{bmatrix} + \begin{bmatrix} 0 \\ 0 \\ I_4 \end{bmatrix} \Delta u(k) + \begin{bmatrix} I_4 \\ 0 \\ 0 \end{bmatrix} \Delta y_{ref\_c}(k+1)$$

$$X_D(k+1) = \Phi X_D(k) + G\Delta u(k) + G_R \Delta y_{ref\_c}(k+1) \tag{4}$$

where Δ refers to the difference between the values corresponding to the present sampling time with that of the preceding sampling time.

A performance index J is defined as follows:

$$J = \sum_{k=1}^{\infty} \left[X_D^T(k) Q X_D(k) + \Delta u^T(k) H \Delta u(k) \right] \tag{5}$$

where, $Q \in R^{11\cdot 11}$ and $H \in R^{4\cdot 4}$ are the weighting factor matrices. According to optimal regulator theory, $\Delta u(k)$ is derived by solving eq.(4), such that (5) is minimized.

$$\left.\begin{aligned} \Delta u(k) &= F_D X_D(k) + F_{DR} \Delta R(k+1) \\ &= F_{De} e_C(k) + F_{Dx} \Delta x(k) \\ &\quad + F_{Du} \Delta u(k-1) + F_{DR} \Delta y_{ref\_c}(k+1) \\ F_D &= -\left[H + G^T P G \right]^{-1} G^T P \Phi \left[\Phi \quad G \right] \\ &= F_0 \left[\Phi \quad G \right] \\ F_{DR} &= F_0 G_R \\ P &= Q + \Phi^T P \Phi - \Phi^T P G \left[H + G^T P G \right]^{-1} G^T P \Phi \end{aligned}\right\} \tag{6}$$

Since the futuristic reference values are known a priori, a preview control term is added to improve the overall response of the control system. On the basis of (6), the Improved Digital Optimal Type-1 Servo system is illustrated in Fig. 3.

4. SIMULATION RESULTS

Table1 shows simulation parameters for the new GC amplifier in MRI systems. The latest switching devices (IGBT, Power MOSFET, etc.) are not sufficiently equipped to operate the GC current since their switching frequencies are limited in order to guard itself

Table 1 Simulation parameter

3Φ Power Source Voltage		$v_{3ph\ r.m.s.}$	500[V]
Sampling Frequency		f_S	20.0[kHz]
Gradient Coil	Inductance	L_{GC}	200[μH]
	Resistance	r_{GC}	0.1[Ω]
4 Quadrant DC Chopper	Inductance	L_{a1}~L_{b2}	180[μH]
	Capacitance	C_a, C_b	5.0[μH]
	Resistance	R_{Ca}, R_{Cb}	1.0[Ω]

from device destruction. For example, IGBT which is widely used has an operation frequency of 20[kHz]. Therefore, each IGBT gate signal instruction is given 1 command per 50[μs] (Sampling Frequency=20[kHz]). The DC chopper inductor current will be considered which has the same ripple frequency as the switching frequency (20kHz), but the current ripple frequency of Gradient Coil will be twice the switching frequency owing to optimal gate signal layouts (Fig. 2).

Figure 4 shows the input 3Φ DC voltage (v_{3ph}) and the input voltage (v_{in}) which has eliminated high frequency ripples. The 6-diode full-wave rectifiable circuit changes 3Φ-AC to DC with a large ripple frequency of about 360 [Hz]. Because of filtering by the large filter capacitor C_f (over 1.0[mF]), v_{in} can be kept a constant value of about 700[V].

Figure 5 shows a GC current along with a trapezoidal reference wave form, having a rate of increase of 1.0[A] per 1.0[μs] and a 250[A] flat top maximum current. By taking a broad view of the GC current as shown in this figure, it could be understood that the current follows the target with almost no delay time which confirms the high controllability of the new digital optimal type-1 controller. It is clear from Fig.6 that the tracking is excellent for various target currents.

Figure 7(a) shows the magnification of the GC current flat top of Fig. 5. Observing Fig. 7(a) closely, the GC current has only a little overshoot at the transition point to the fixed current target, and converge thereafter with a small oscillation. The efficacy of the corrective value $R_d(k)$ is appreciated as compared with Fig. 7(b), where no corrective value has been used. The GC current in Fig. 7(b) has a steady-state deviation when the steady current target and has a large current overshoot than Fig. 7(a). Consequently from these observations it is evident that using the corrective value $R_d(k)$ enhance the controllability of the GC current.

Figure 8 shows the simulation result of the input

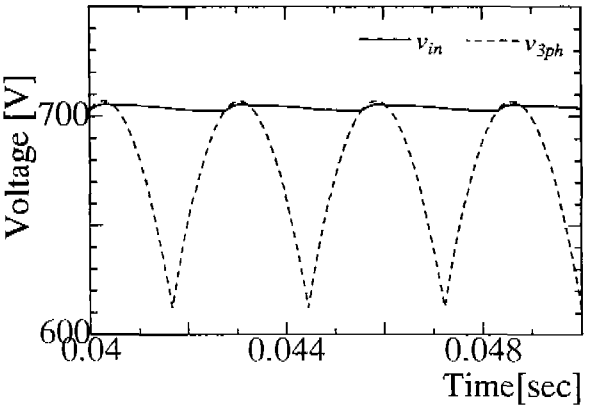

Fig.4 Input Voltage Waveforms

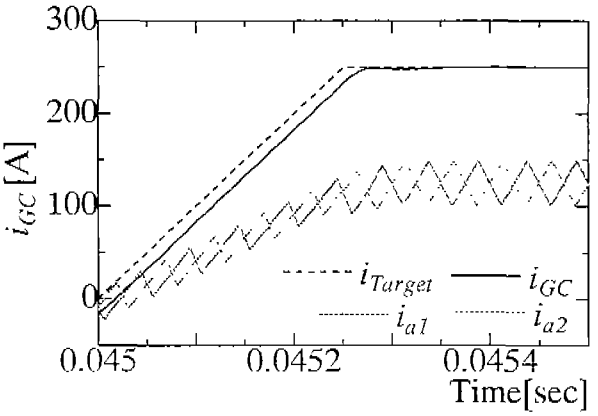

Fig.5 Tracking quality of GC current for a trapezoidal reference wave form

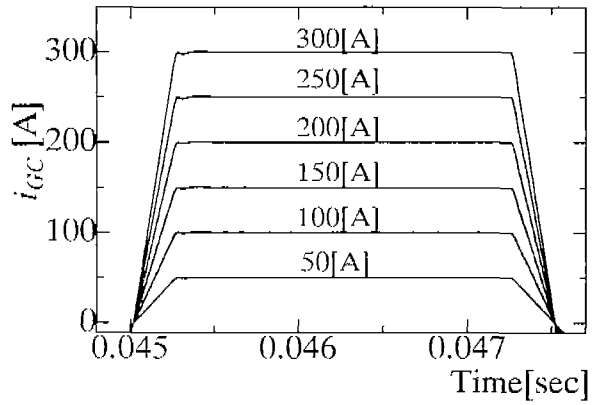

Fig.6 GC currents for several targets

current (i_{in}) for the proposed circuit for two different values of the circuit parameters r_{GC} . If this figure is closely looked at it indicates the flow of the input-output power. In other words, the positive current means the consumption power in the proposed circuit, and the negative means the regenerative power to the input filter capacitor. According to these simulation results, the proposed amplifier consumes a large amount of power with the increase of the internal resistance r_{GC} as

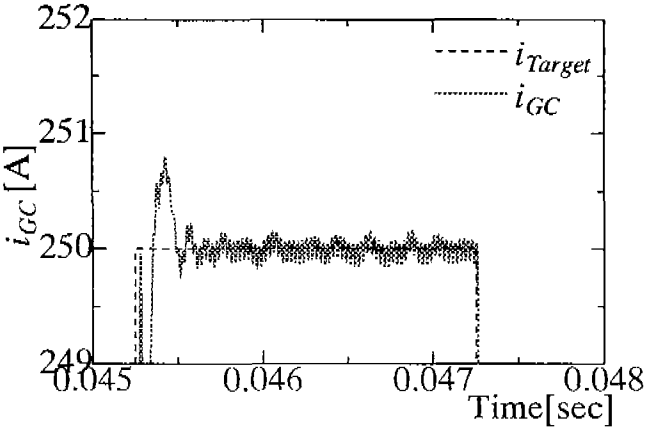

(a) The large scale GC current based on the optimal controller with corrective value R_C(k)

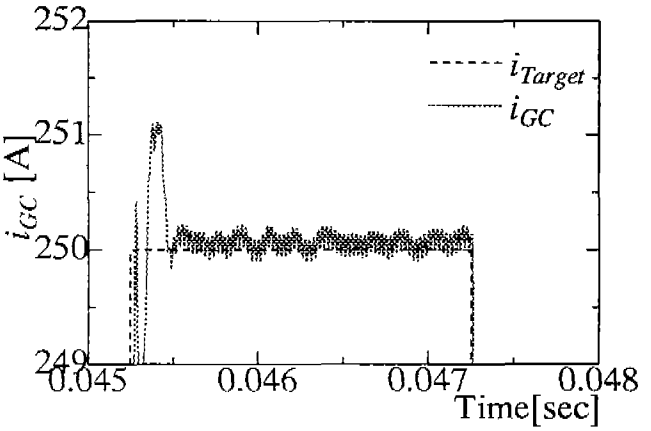

(b) The large scale GC current based on the optimal controller with no corrective value

Fig.7 The comparison of GC current for R_C(k)

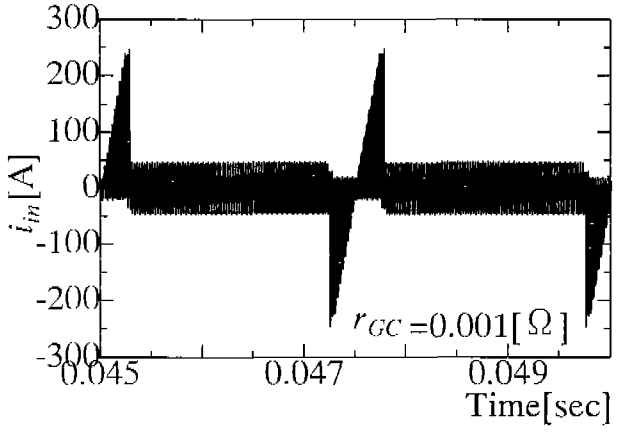

(a) The input current condition for small r_{GC}

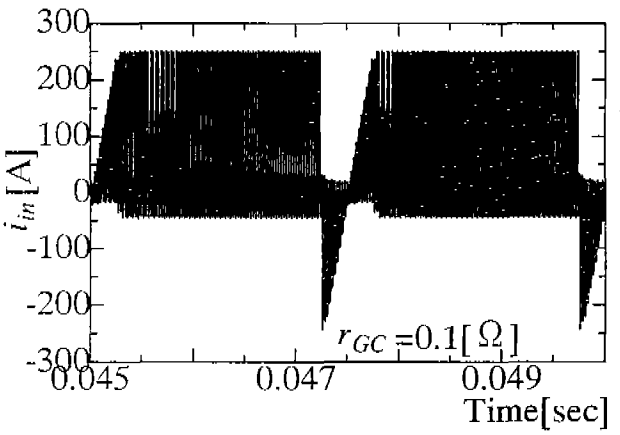

(b) The input current condition for large r_{GC}

Fig.8 The compensation of the input current for r_{GC}

expected. The ideal condition of Gradient Coil and chopper inductor do not have the internal resistance, but in reality, both have a small resistance. This consumption power is dissipated as a heat energy in MRI systems. Figure 9 gives the power loss in proposed amplifier. Since the MRI system is expected to generate heat, we have to study how to eliminate the heat.

5. CONCLUSIONS

A two-paralleled 4-quadrant DC chopper type power conversion circuit using IGBTs has been introduced into the switch-mode gradient power amplifiers in MRI systems in order to overcome the limitation of low frequency switching characteristics and to obtain high speed and precise controllability. A unique digital control scheme to minimize the ripple

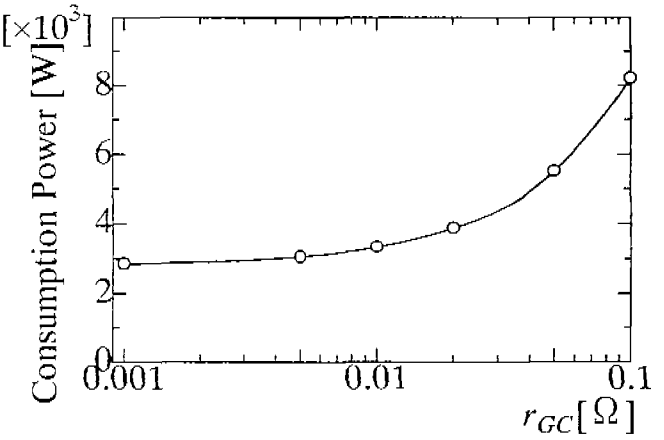

Fig.9 Consumption power of the proposed amplifier

and improve the rise/fall response characteristics of the output current in the GC has also been proposed. The input voltage v_{in} has a ripple with the 3-phase rectification of AC to DC, but the controlled current has eliminated the

negative effect and tracks the target current well despite sharp variations in the target current. Moreover, it has been proved by this simulation that the proposed control method with the corrective value $R_C(k)$ is very useful to improve the GC current controllability for the proposed circuit. It can reduce the steady-state deviation of the GC current and the current overshoot for the target. We can also build the new controller with artificial intelligent concepts such as Fuzzy, Neural Network, and GA (Generic Algorithms) etc..

On the other, the important problem was found out by the estimation of the power loss. The inductor current conduction will reduce in proportion to the rising temperature. In other words, the circuit efficiency will reduce if we should not consider the elimination of heat during the experiment phase.

In conclusion, the new power conversion circuit using digital optimal control scheme can be applied to many industrial equipment with highly-inductive magnetic coils. The simulation results through computer-aided analysis confirm that a high GC-current tracking accuracy is achieved under high power output levels in this system.

6. REFERENCES

[1] K.P.Gokhale, A.Kawamura, and R.G.Hoft, 1987, "Dead Beat Microprocessor Control of PWM Inverter for Sinusoidal Output Waveforms Synthesis", IEEE-Trans. Industry Applications, pp. 901-910

[2] A.Kawamura, T.Haneyoshi, and R.G.Hoft, 1988, "Deadbeat Controlled PWM Inverter with Parameter Estimation Using Only Voltage Sensor", IEEE-Trans. Power Electronics, pp.118-125

[3] K.Siri and C.Q-Lee, 1990,"Current Distribution Control of Converters Connected in Parallel", Records of IEEE-IAS, pp.1274-1280

[4] Copley Controls Corp., 1991, "Extending the Scope of PWM Amplifiers", PCIM-Europe Magazine, pp.182-184

[5] H.Fukuda and M.Nakaoka, 1994, "State-Vector Feedback 100kHz Carrier PWM Power Amplifier for High-Precision Magnetic-Field Current Pattern Tracking", Proceedings of IEE-PEVD, pp.211-216

[6] H.Fukuda and M.Nakaoka, 1995, "High-Frequency ZVS PWM Power Amplifier for Magnetic-Field Current Tracking Control Scheme and Its Design Considerations", Proceedings of IEEE-PEDS, pp.238-245

[7] S.Watanabe, P.Boyagoda, M.Nakaoka, and H.Takano, 1997, "Advanced Digital Control Scheme of A Paralleled Bridge Type Current Tracking High Power Conversion Amplifier for Magnetic Resonance Imaging", Proceedings of IEE EPE'97,Vol.2, pp.297-302